

# A residual error estimator for the XFEM approximation of the elasticity problem

Patrick Hild <sup>1</sup>, Vanessa Lleras <sup>1</sup>, Yves Renard <sup>2</sup>

<sup>1</sup> Laboratoire de Mathématiques de Besançon, UMR CNRS 6623  
Université de Franche-Comté, 16 route de Gray, 25030 Besançon, France.

e-mail: patrick.hild@univ-fcomte.fr, vanessa.lleras@univ-fcomte.fr

<sup>2</sup> Université de Lyon, CNRS,  
INSA-Lyon, ICJ UMR5208, LaMCoS UMR5259, F-69621, Villeurbanne, France.

e-mail: yves.renard@insa-lyon.fr

September 1, 2009

## Abstract

In this work we propose, analyse and implement a residual a posteriori error estimator for the elasticity system in two space dimensions approximated by the eXtended Finite Element Method (XFEM). The XFEM allows to perform finite element computations on multi-cracked domains using meshes of the non-cracked domain by adding supplementary basis functions of Heaviside type and singular functions in order to take into account the crack geometry and the singularity at the crack tip respectively.

**Key words:** elasticity, eXtended Finite Element Method, cracked domain, error estimators, residuals.

**Abbreviated title:** XFEM residual estimators in elasticity.

**MOS subject classification:** 65N30, 65N15

## 1 Introduction and notation

The eXtended Finite Element Method (XFEM) was initially introduced in [24, 23] (in the linear elasticity context) in order to avoid remeshing in domains with evolutionary cracks. The idea of the method is to enrich the classical finite element basis with both non-smooth functions representing the singularities at the reentrant corners (as in the singular enrichment method introduced in [30]) and also with step functions (of Heaviside type) along the crack since the finite element mesh does not coincide with the cracked domain. After numerous numerical works developed in various contexts of mechanics, the first convergence results with a priori error estimates were recently obtained in [9, 10]: in the convergence analysis, a difficulty consists in evaluating the local error in the elements cut by the crack by using appropriate extension operators and specific estimates. In the latter references, the authors obtain an error estimate of order  $h$  ( $h$  denotes the discretization parameter) with a  $H^{2+\varepsilon}$  regularity assumption on the regular part of the solution keeping in mind that the solution is only  $H^{3/2-\varepsilon}$  regular for any positive  $\varepsilon$ . A more recent work in [25] proves an

optimal error estimate of order  $h$  under a  $H^2$ -regularity hypothesis of the regular part of the solution.

Some remarkable numerical work has been performed on a posteriori error estimation for XFEM. A simple derivative recovery technique and its associated a posteriori error estimator have been proposed in [5], [6], [7] and [27]. These recovery based a posteriori error estimations outperform the superconvergent patch recovery technique (SPR) introduced by Zienkiewicz and Zhu. In the present work, we propose and analyze an error estimator of residual type (see [2] for the early ideas and analyzes and e.g., [31] and the references therein for a more complete overview) for the XFEM applied to the linear elasticity system. Since the meshes do not coincide with the domain near the crack we need to introduce and to study a specific quasi-interpolation operator of averaging type (see e.g., [3, 11, 13, 20, 28, 29] for various averaging type operators). The use of such an operator allows us to obtain an upper bound of the discretization error. In the last section, we present several numerical results, achieved with the finite element library Getfem++ ([26]). The numerical experiments show that the error estimator and the discretization error admit similar convergence rates as the discretization parameter vanishes.

We introduce some useful notation and several functional spaces. As usual, we denote by  $(L^2(\cdot))^d$  and by  $(H^s(\cdot))^d$ ,  $s \geq 0$ ,  $d = 1, 2$  the Lebesgue and Sobolev spaces in one and two space dimensions (see [1]). The usual norm of  $(H^s(D))^d$  is denoted by  $\|\cdot\|_{s,D}$  and we keep the same notation when  $d = 1$  or  $d = 2$ . For shortness the  $(L^2(D))^d$ -norm will be denoted by  $\|\cdot\|_D$  when  $d = 1$  or  $d = 2$ . In the sequel the symbol  $|\cdot|$  will denote either the Euclidean norm in  $\mathbb{R}^2$ , or the length of a line segment, or the area of a plane domain. Finally the notation  $a \lesssim b$  means here and below that there exists a positive constant  $C$  independent of  $a$  and  $b$  (and of the mesh size of the triangulation) such that  $a \leq C b$ . The notation  $a \sim b$  means that  $a \lesssim b$  and  $b \lesssim a$  hold simultaneously.

## 2 The elasticity problem on a cracked domain

Let  $\Omega$  be an open subset of  $\mathbb{R}^2$  having a crack, with a polygonal boundary  $\partial\Omega$  where  $\Gamma_C \subset \partial\Omega$  denotes the crack (the crack  $\Gamma_C$  consists of two distinct straight line segments having the same location). We consider a ‘‘partition’’ of  $\partial\Omega$  into three open disjoint subsets  $\Gamma_D$ ,  $\Gamma_N$  and  $\Gamma_C$  so that  $\partial\Omega = \bar{\Gamma}_D \cup \bar{\Gamma}_N \cup \bar{\Gamma}_C$ . An homogeneous Dirichlet condition is prescribed on  $\Gamma_D$  and an homogeneous Neumann condition holds on  $\Gamma_N \cup \Gamma_C$ . The homogeneous conditions on  $\Gamma_D$  and  $\Gamma_N$  are chosen to simplify and the extension to the nonhomogeneous case is straightforward. We further suppose that the measures of  $\Gamma_D$  and  $\Gamma_C$  are positive (see Figure 1).

In this paper we consider the elasticity problem: for  $f \in (L^2(\Omega))^2$  let  $u$  be the displacement field solution to

$$(1) \quad \begin{cases} -\operatorname{div} \sigma(u) &= f & \text{in } \Omega, \\ u &= 0 & \text{on } \Gamma_D, \\ \sigma(u)n &= 0 & \text{on } \Gamma_N \cup \Gamma_C, \end{cases}$$

where  $\sigma(u) = C\varepsilon(u)$  denotes the stress tensor field obtained from the elasticity operator  $C$  and from the linearized strain tensor field  $\varepsilon(u) = (\nabla u + \nabla u^T)/2$  and  $n$  stands for the unit outward normal on  $\partial\Omega$ . Set

$$V = \{v \in (H^1(\Omega))^2 : v = 0 \text{ on } \Gamma_D\}.$$

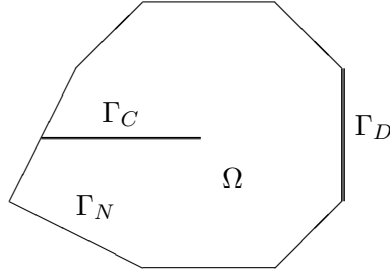


Figure 1: The geometry of the cracked domain  $\Omega$

Then, the variational solution of (1) is the unique solution  $u$  of

$$(2) \quad u \in V, \quad \int_{\Omega} \sigma(u) : \varepsilon(v) \, dx = \int_{\Omega} f \cdot v \, dx, \quad \forall v \in V,$$

where the notation  $\cdot$  (resp.  $:$ ) stands for the inner product in  $\mathbb{R}^2$  (resp. in the space of second order symmetric tensors of  $\mathbb{R}^2$ ). The solution  $u$  to the elasticity problem can be written as a sum of a regular part  $u_r$  and a singular part  $u_s = K_I u_I + K_{II} u_{II}$  where  $K_I$  and  $K_{II}$  are the stress intensity factors (see for instance [22]) and the functions  $u_I$  and  $u_{II}$  are defined in polar coordinates  $(r, \theta)$  as follows in the case of an horizontal crack with a crack tip at the right extremity (as in Figure 1):

$$(3) \quad u_I = \frac{\lambda + \mu}{\mu(3\lambda + 2\mu)} \sqrt{\frac{r}{2\pi}} \begin{pmatrix} \cos \frac{\theta}{2} \\ \sin \frac{\theta}{2} \end{pmatrix} (a + b \cos \theta),$$

$$(4) \quad u_{II} = \frac{\lambda + \mu}{\mu(3\lambda + 2\mu)} \sqrt{\frac{r}{2\pi}} \begin{pmatrix} \sin \frac{\theta}{2} (c + 2 + \cos \theta) \\ \cos \frac{\theta}{2} (2 - c - \cos \theta) \end{pmatrix}.$$

In the previous definition  $r$  denotes the distance to the crack tip,  $\lambda$  and  $\mu$  are the Lamé coefficients and

$$a = 2 + \frac{2\mu}{\lambda + 2\mu}, \quad b = -2 \frac{\lambda + \mu}{\lambda + 2\mu}, \quad c = \frac{\lambda + 3\mu}{\lambda + \mu}.$$

Note that the normal (resp. tangential) component of  $u_I$  (resp.  $u_{II}$ ) is discontinuous across the crack (i.e.,  $\theta = \pi$ ). It can be checked that for any positive  $\varepsilon$ , the functions  $u_I$  and  $u_{II}$  lie in  $(H^{\frac{3}{2}-\varepsilon}(\Omega))^2$  (see, e.g. [17, 18]).

### 3 Discretization of the elasticity problem with the XFEM

We approximate problem (1) by the so called XFEM (eXtended Finite Element Method) introduced in [24]. Namely we consider a regular family of triangulations  $T_h, h > 0$  of the noncracked domain made of closed triangles  $T$  such that  $\bar{\Omega} = \cup_{T \in T_h} T$  (see [8, 12, 14]). For  $T \in T_h$  we recall that  $h_T$  is the diameter of  $T$  and  $h = \max_{T \in T_h} h_T$ . The regularity of the mesh implies in particular that for any edge  $E$  of  $T$  one has  $h_E = |E| \sim h_T$ . Since the

triangles in  $T_h$  do not coincide with the crack we define the family of generalized elements  $G_h, h > 0$  containing the following elements (see Figure 2):

- the triangles in  $T \in T_h$  whose interior does not intersect  $\Gamma_C$ ,
- the (non closed) triangles and quadrangles obtained when the crack cuts (into two parts) a triangle in  $T_h$ ,
- the (non closed) cracked triangle containing the crack tip.

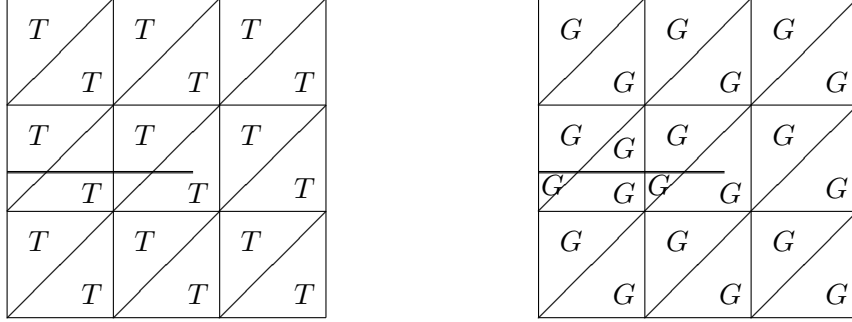


Figure 2: Standard elements  $T \in T_h$  and generalized elements  $G \in G_h$

This implies that  $\bar{\Omega} = \cup_{G \in G_h} \bar{G}$  and  $\cup_{G \in G_h} \overset{\circ}{G} \subset \Omega$  where  $\overset{\circ}{G}$  denotes the interior of  $G$ . We next give an important definition:

**Definition 3.1** Let  $\mathcal{N}_h$  be the set of nodes of the triangulation  $T_h$ . We say that a node  $x \in \mathcal{N}_h$  is enriched if the patch  $\omega_x$  surrounding  $x$ :  $\omega_x = \cup_{T:x \in T} T$  is cut in (at least) two subsets by the crack (see Figure 3) and we denote by  $\mathcal{N}_h^H \subset \mathcal{N}_h$  the set of enriched nodes. We say that a triangle  $T \in T_h$  is enriched (resp. partially enriched) if its three nodes (resp. one or two nodes) are enriched.

We denote by  $h_x$  the diameter of the patch  $\omega_x$ . If  $T \in T_h$  we denote by  $\omega_T$  the union of all elements in  $T_h$  having a nonempty intersection with  $T$ . Similarly for a edge  $E$  of a triangle in  $T_h$  we denote by  $\omega_E$  the union of all elements in  $T_h$  having a nonempty intersection with  $\bar{E}$ . Set  $\mathcal{N}_h^D = \mathcal{N}_h \cap \bar{\Gamma}_D$  (note that the extreme nodes of  $\bar{\Gamma}_D$  belong to  $\mathcal{N}_h^D$ ).

Let  $E_h$  denote the set of edges of the elements in  $G_h$  (the edges are supposed to be relatively open) and  $E_h^{int} = \{E \in E_h : E \subset \Omega\}$  be the set of interior edges of  $G_h$ ,  $E_h^{ext} = E_h \setminus E_h^{int}$ . We denote by  $E_h^N = \{E \in E_h : E \subset \Gamma_N\}$ ,  $E_h^C = \{E \in E_h : E \subset \Gamma_C\}$  the set of exterior edges included into the part of the boundary where the Neumann condition is prescribed. For a generalized element  $G \in G_h$  (resp. standard element  $T \in T_h$ ), we will denote by  $E_G$  the set of edges of  $G$  (resp., by  $E_T$  the set of edges of  $T$ ) and according to the above notation, we set  $E_G^{int} = E_G \cap E_h^{int}$ ,  $E_G^N = E_G \cap E_h^N$ ,  $E_G^C = E_G \cap E_h^C$ . For each edge  $E \in E_h$  we fix one of the two normal vectors to the element and we denote it by  $n_E$ . The jump of some scalar or vector valued function  $v$  across an edge  $E \in E_h$  at a point  $y \in E$  is defined as

$$[[v(y)]]_E = \begin{cases} \lim_{\alpha \rightarrow 0^+} v(y + \alpha n_E) - v(y - \alpha n_E) & \forall E \in E_h^{int}, \\ v(y) & \forall E \in E_h^{ext}. \end{cases}$$

The main idea of the extended finite element method is to enrich the classical finite element space by:

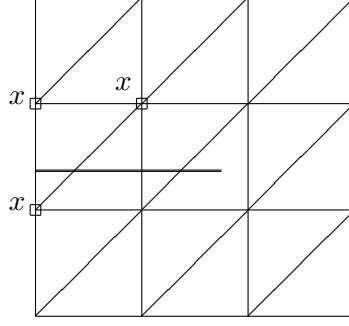


Figure 3: Enriched nodes  $x \in \mathcal{N}_h^H$

- singular functions at the crack tip in order to take into account the singularity of the displacement field,
- discontinuous functions located along the crack in order to take into account the discontinuity of the solution across the crack.

Following [24], the singular functions at the crack tip are constructed using the four singular basis functions:

$$\begin{aligned}
 F_1 &= \sqrt{r} \sin(\theta/2), \\
 F_2 &= \sqrt{r} \cos(\theta/2), \\
 F_3 &= \sqrt{r} \sin(\theta) \sin(\theta/2), \\
 F_4 &= \sqrt{r} \sin(\theta) \cos(\theta/2).
 \end{aligned}$$

The discontinuous functions are constructed from a Heaviside like function  $H$  which is equal to 1 on one side (of the straight extension, see Figure 4) of the crack and to  $-1$  on the other side. This allows the following definition of the extended finite element space:

$$(5) \quad V_h = \left\{ v_h \in (C(\Omega))^2 : v_h = \sum_{x \in \mathcal{N}_h} a_x \lambda_x + \sum_{x \in \mathcal{N}_h^H} b_x H \lambda_x + \chi \sum_{i=1}^4 c_i F_i \right. \\
 \left. = v_{h,r} + \chi v_{h,s}, \quad a_x, b_x, c_i \in \mathbb{R}^2 \right\} \subset V,$$

where  $\lambda_x$  denotes the classical finite element  $P_1$  shape functions at node  $x \in \mathcal{N}_h$  satisfying  $\lambda_x(x') = \delta_{x,x'}$ , for any  $x' \in \mathcal{N}_h$  and  $\chi \in C^2(\bar{\Omega})$  is a cutoff function satisfying

$$(6) \quad \chi(r) = \begin{cases} 1 & \text{if } r \leq r_0, \\ \rho \in (0, 1) & \text{if } r_0 < r < r_1, \\ 0 & \text{if } r \geq r_1, \end{cases}$$

where  $r$  denotes the the distance to the crack tip and  $r_0$  and  $r_1$  are given positive numbers such that  $r_0 < r_1$ . Such a cutoff function  $\chi$  was introduced in [9, 10] in order to improve the performances (in terms of convergence) of the original method in [24].

The finite element approximation of (2) consists of finding  $u_h$  such that

$$(7) \quad u_h \in V_h, \quad \int_{\Omega} \sigma(u_h) : \varepsilon(v_h) dx = \int_{\Omega} f \cdot v_h dx, \quad \forall v_h \in V_h.$$

Note that Lax-Milgram Lemma implies the existence of a unique solution to problem (7).

**Remark 3.2** *A quasi-optimal a priori error estimate is obtained in [9, 10] for the XFEM involving the cutoff function  $\chi$ . Under a  $(H^{2+\varepsilon}(\Omega))^2$  regularity assumption for  $u - \chi u_s$  (for some positive  $\varepsilon$ ), the authors prove that  $\|u - u_h\|_{1,\Omega} \lesssim h \|u - \chi u_s\|_{2+\varepsilon,\Omega}$ . This result has been recently improved in [25] where a convergence of order  $h$  is proved with  $(H^2(\Omega))^2$  regularity for  $u - \chi u_s$ . Note that when using a classical finite element method one obtains a convergence rate of only  $h^{1/2-\varepsilon}$  since  $u$  lies in  $(H^{3/2-\varepsilon}(\Omega))^2$  for any  $\varepsilon > 0$ .*

## 4 The quasi-interpolation operator

The aim of this section is to introduce a quasi-interpolation operator which will be used in the forthcoming a posteriori error analysis. This operator was already considered by the authors in [21] and we recall its properties to render the paper self contained.

### 4.1 Definition

Quasi-interpolation operators of averaging type are a common tool for residual a posteriori error analysis (see e.g., [3, 11, 13, 20, 28, 29] for various operators). At a node  $x$ , the value of the quasi-interpolation is often an "average" of the function on the patch  $\omega_x$  surrounding  $x$ . To simplify the forthcoming discussion we suppose (as in Figure 1) that the end points of the crack belonging to  $\partial\bar{\Omega}$  are not submitted to Dirichlet conditions. For the sake of simplicity, we first build the quasi-interpolation operator  $\pi_h$  in the scalar case: let us set

$$X = \{v \in H^1(\Omega) : v = 0 \text{ on } \Gamma_D\}.$$

and

$$X_h = \left\{ v_h \in C(\Omega) : v_h = \sum_{x \in \mathcal{N}_h} \alpha_x \lambda_x + \sum_{x \in \mathcal{N}_h^H} \beta_x H \lambda_x, \quad \alpha_x, \beta_x \in \mathbb{R} \right\} \subset X.$$

The quasi-interpolation operator  $\pi_h$  will be defined as

$$\pi_h : X \rightarrow X_h.$$

**Remark 4.1** *Note that  $X_h$  does not involve any singular function at the crack tip.*

The first idea would be to use such an operator on the regular mesh  $T_h$ . In such an approach, terms such as  $\|u - u_h\|_{1,\omega_T}$  (where  $T \in T_h$ ) do appear and unfortunately  $u$  and  $u_h$  do not lie in  $(H^1(\bar{\Omega}))^2$  (hence  $u - u_h$  does in general not lie in  $(H^1(\omega_T))^2$ ) due to the discontinuity across the crack.

A second idea would be to define  $\pi_h v$  (with  $v \in H^1(\Omega)$ ) separately on each side of the crack. If we divide  $\Omega$  into  $\Omega_1$  and  $\Omega_2$  using the crack and a straight extension of the crack (see Figure 4) one could first try to define  $\pi_h v$  on  $\Omega_1$  (resp.  $\Omega_2$ ) by using the only values of  $v$  on  $\Omega_1$  (resp.  $\Omega_2$ ). This consists of defining  $\pi_h v$  on each generalized element  $G \in G_h$ . It is easy to see that this approach leads to technical difficulties since the elements in  $G_h$  are sometimes quadrangles.

As a consequence, we choose an approach which consists in determining  $\pi_h v$  separately on each side of the crack by defining  $\pi_h v|_G$ ,  $G \in G_h$  and by using the values of  $v$  on both sides of the crack. This leads us to use extension operators.

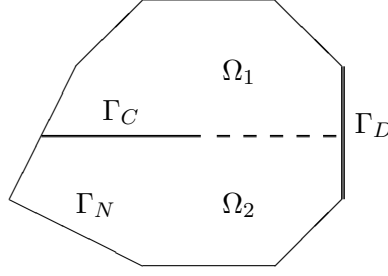


Figure 4: Domain decomposition using a straight extension of the crack

As already mentioned, let us divide  $\Omega$  into  $\Omega_1$  and  $\Omega_2$  using the crack and a straight extension of the crack (see Figure 4). Let  $v \in H^1(\Omega)$  and let  $v_1 = v|_{\Omega_1} \in H^1(\Omega_1)$  and  $v_2 = v|_{\Omega_2} \in H^1(\Omega_2)$  be the restrictions of  $v$  on  $\Omega_1$  and  $\Omega_2$ , respectively. Let us consider an extension of  $v_1$  defined on  $\bar{\Omega}$  (see [1, 15]) denoted  $\tilde{v}_1$  such that

$$(8) \quad \|\tilde{v}_1\|_{1,\bar{\Omega}} \lesssim \|v_1\|_{1,\Omega_1} \leq \|v\|_{1,\Omega}$$

and an extension  $\tilde{v}_2$  (defined on  $\bar{\Omega}$ ) of  $v_2$  such that

$$(9) \quad \|\tilde{v}_2\|_{1,\bar{\Omega}} \lesssim \|v_2\|_{1,\Omega_2} \leq \|v\|_{1,\Omega}.$$

For any  $v \in H^1(\Omega)$ , we define  $\pi_h v$  as the unique element in  $X_h$

$$(10) \quad \pi_h v = \sum_{x \in \mathcal{N}_h} \alpha_x(v) \lambda_x + \sum_{x \in \mathcal{N}_h^D} \beta_x(v) H \lambda_x,$$

satisfying the following conditions:

- Step 1. Definition of  $\pi_h v$  at the nodes  $\mathcal{N}_h$  of the triangulation  $T_h$ .
  - (i) (not enriched nodes) If  $x \in \mathcal{N}_h \setminus \mathcal{N}_h^D$  is such that  $\omega_x$  is not cut (i.e., not divided into more than one part) by the crack then

$$\pi_h v(x) = \frac{1}{|\omega_x|} \int_{\omega_x} v(y) dy.$$

From Cauchy-Schwarz inequality, we get

$$|\pi_h v(x)| \lesssim |\omega_x|^{-1/2} \|v\|_{\omega_x} \sim h_x^{-1} \|v\|_{\omega_x} \leq h_x^{-1} \|v\|_{\omega_x} + \|\nabla v\|_{\omega_x}.$$

Note that the three nodes of the triangle containing the crack tip are concerned with the latter case (see Figure 3).

- (ii) (enriched nodes) If  $x \in \mathcal{N}_h \setminus \mathcal{N}_h^D$ ,  $x \in \bar{\Omega}_\ell$ ,  $\ell = 1, 2$ , is such that  $\omega_x$  is cut by the crack then we set

$$\pi_h v(x) = \frac{1}{|\omega_x|} \int_{\omega_x} \tilde{v}_\ell(y) dy.$$

We deduce

$$|\pi_h v(x)| \lesssim |\omega_x|^{-1/2} \|\tilde{v}_\ell\|_{\omega_x} \sim h_x^{-1} \|\tilde{v}_\ell\|_{\omega_x} \leq h_x^{-1} \|\tilde{v}_\ell\|_{\omega_x} + \|\nabla \tilde{v}_\ell\|_{\omega_x}.$$

Note that if  $x$  lies on the crack and (ii) is satisfied then there are two possible values for  $\pi_h v(x)$ : one corresponding to  $\pi_h v(x)$  on  $\bar{\Omega}_1$  and the other one to  $\pi_h v(x)$  on  $\bar{\Omega}_2$ . See step 2 for the determination of  $\pi_h$  in this case.

- (iii) If  $x \in \mathcal{N}_h^D$ , denote  $\Gamma_x = \omega_x \cap \Gamma_D$  (recall that  $\bar{\Gamma}_C \cap \bar{\Gamma}_D = \emptyset$  to simplify the discussion) and set:

$$\pi_h v(x) = \frac{1}{|\Gamma_x|} \int_{\Gamma_x} v(y) d\Gamma.$$

By using a scaled trace inequality (see, e.g., [17, 19]):

$$(11) \quad \|v\|_E \lesssim h_E^{-1/2} \|v\|_T + h_E^{1/2} \|\nabla v\|_T, \quad \forall v \in H^1(T), \forall T \in T_h, \forall E \in E_T,$$

we get

$$\begin{aligned} |\pi_h v(x)| &\lesssim |\Gamma_x|^{-1/2} \|v\|_{\Gamma_x} \sim h_x^{-1/2} \|v\|_{\Gamma_x} \lesssim h_x^{-1/2} \left( h_x^{-1/2} \|v\|_{\omega_x} + h_x^{1/2} \|\nabla v\|_{\omega_x} \right) \\ &\lesssim h_x^{-1} \|v\|_{\omega_x} + \|\nabla v\|_{\omega_x}. \end{aligned}$$

- Step 2. Definition of  $\pi_h v$  on  $\Omega$ .

With the previous nodal expressions we define by linear interpolation the function  $\pi_h v$  on any triangle  $T \in T_h$  excepted those cut by the crack. Note that a triangle can be totally enriched (i.e., its three nodes are enriched) and not cut by the crack. If the triangle is cut by the crack then it is either enriched (three nodes enriched) or partially enriched (one or two enriched nodes). The definition on the triangles cut by the crack is given hereafter.

Consider first a totally enriched triangle  $T$  with e.g.,  $x_1 \in \Omega_1$  and  $x_2, x_3 \in \Omega_2$ . In order to determine  $(\pi_h v)|_{\Omega_1 \cap T}$ , we write:

$$(12) \quad \tilde{\pi}_h^1 v(x) = \frac{1}{|\omega_x|} \int_{\omega_x} \tilde{v}_1(y) dy.$$

for  $x = x_1, x_2, x_3$ . Then  $\tilde{\pi}_h^1 v$  is defined by linear interpolation on  $T$  and then  $\pi_h v$  is defined on  $T \cap \Omega_1$  as the restriction of  $\tilde{\pi}_h^1 v$  on  $T \cap \Omega_1$ .

Similarly we define  $(\pi_h v)|_{\Omega_2 \cap T}$  to be the restriction on  $T \cap \Omega_2$  of  $\tilde{\pi}_h^2 v$  defined for  $x = x_1, x_2, x_3$  by

$$(13) \quad \tilde{\pi}_h^2 v(x) = \frac{1}{|\omega_x|} \int_{\omega_x} \tilde{v}_2(y) dy.$$

A similar construction is achieved for the partially enriched triangles: if a node  $x$  is not enriched then we compute the value of  $\pi_h v(x)$  at this node and if it is enriched then we compute both quantities (12) and (13) corresponding to  $\tilde{v}_1$  and  $\tilde{v}_2$  at this node.



**Remark 4.2** From the previous construction of  $\pi_h v$  and expression (10) we see that  $\alpha_x(v) = \pi_h v(x)$  if  $x \in \mathcal{N}_h \setminus \mathcal{N}_h^H$ . If  $x \in \mathcal{N}_h^H$ ,  $x \in \bar{\Omega}_k$  and denoting  $\ell = 3 - k$ , we have

$$\alpha_x(v) + \beta_x(v)H(x) = \frac{1}{|\omega_x|} \int_{\omega_x} \tilde{v}_k(y) dy, \quad \text{and} \quad \alpha_x(v) - \beta_x(v)H(x) = \frac{1}{|\omega_x|} \int_{\omega_x} \tilde{v}_\ell(y) dy.$$

Hence

$$\alpha_x(v) = \frac{1}{2|\omega_x|} \int_{\omega_x} (\tilde{v}_k(y) + \tilde{v}_\ell(y)) dy, \quad \text{and} \quad \beta_x(v) = \frac{H(x)}{2|\omega_x|} \int_{\omega_x} (\tilde{v}_k(y) - \tilde{v}_\ell(y)) dy.$$

## 4.2 Stability

Next we consider the stability properties of the quasi-interpolation operator on the generalized elements.

**Lemma 4.3** For all  $v \in H^1(\Omega)$  and all  $T \in T_h$  one has:

(i) if none of the nodes of  $T$  is enriched (so the crack does not cut  $T$ ) then:

$$\|\pi_h v\|_T \lesssim \|v\|_{\omega_T} + h_T \|\nabla v\|_{\omega_T},$$

(ii) if the three nodes of  $T$  are enriched, then for  $\ell = 1$  and  $\ell = 2$ , we have:

$$\|\pi_h v\|_{T \cap \Omega_\ell} \lesssim \|\tilde{v}_\ell\|_{\omega_T} + h_T \|\nabla \tilde{v}_\ell\|_{\omega_T},$$

(iii) if one or two nodes of  $T$  are enriched and if  $\omega_T$  is cut by the crack (so  $T \subset \bar{\Omega}_\ell$  for  $\ell = 1$  or  $\ell = 2$ ) we have:

$$\|\pi_h v\|_T \lesssim \|\tilde{v}_\ell\|_{\omega_T} + h_T \|\nabla \tilde{v}_\ell\|_{\omega_T},$$

(iv) if one or two nodes of  $T$  are enriched and if  $\omega_T$  contains the crack tip then for  $\ell = 1$  or  $\ell = 2$ , we have:

$$\|\pi_h v\|_{T \cap \Omega_\ell} \lesssim \|\tilde{v}_\ell\|_{\omega_T} + \|v\|_{\omega_T} + h_T \|\nabla \tilde{v}_\ell\|_{\omega_T} + h_T \|\nabla v\|_{\omega_T}.$$

**Remark 4.4** Due to the mesh regularity there is a mesh independent bounded number of triangles satisfying (iv): more precisely this set is contained in  $\omega_{T^*}$  where  $T^*$  is the triangle containing the crack tip. Some of the triangles in this set are cut by the crack and others no.

**Proof:** (i). If none of the nodes is enriched then for each of the three nodes of  $T$ , we have:

$$|\pi_h v(x)| \lesssim h_x^{-1} \|v\|_{\omega_x} + \|\nabla v\|_{\omega_x}.$$

Writing  $\pi_h v = \sum_{x \in T} \pi_h v(x) \lambda_x$  on  $T$  and using  $\|\lambda_x\|_T \sim h_T \sim h_x$  implies the result.

(ii). Set e.g.,  $\ell = 1$ . Noting that for any of the three nodes of  $T$ , we have

$$|\tilde{\pi}_h^1 v(x)| \lesssim h_x^{-1} \|\tilde{v}_1\|_{\omega_x} + \|\nabla \tilde{v}_1\|_{\omega_x},$$

and using the same estimates as in (i) yields the result. The same result holds when  $\ell = 2$ .

(iii) and (iv). These estimates are obtained as the previous ones.  $\blacksquare$

Now we consider the stability properties of  $\pi_h$  on the edges of the generalized elements not located on the crack.

**Lemma 4.5** For all  $v \in H^1(\Omega)$  and all edge  $E$  of a triangle  $T \in T_h$  one has:  
(i) if both end points of  $E$  are not enriched:

$$\|\pi_h v\|_E \lesssim h_E^{-1/2} \|v\|_{\omega_E} + h_E^{1/2} \|\nabla v\|_{\omega_E},$$

(ii) if both end points of  $E$  are enriched then for  $\ell = 1$  or  $\ell = 2$ , we have:

$$\|\pi_h v\|_{E \cap \bar{\Omega}_\ell} \lesssim h_E^{-1/2} \|\tilde{v}_\ell\|_{\omega_E} + h_E^{1/2} \|\nabla \tilde{v}_\ell\|_{\omega_E},$$

(iii) if only one end point of  $E$  is enriched and if  $\omega_E$  is cut by the crack (so  $E \subset \bar{\Omega}_\ell$  for  $\ell = 1$  or  $\ell = 2$ ), we have:

$$\|\pi_h v\|_E \lesssim h_E^{-1/2} \|\tilde{v}_\ell\|_{\omega_E} + h_E^{1/2} \|\nabla \tilde{v}_\ell\|_{\omega_E},$$

(iv) if only one end point of  $E$  is enriched and if  $\omega_E$  contains the crack tip then for  $\ell = 1$  or  $\ell = 2$ , we have:

$$\|\pi_h v\|_{E \cap \bar{\Omega}_\ell} \lesssim h_E^{-1/2} \|\tilde{v}_\ell\|_{\omega_E} + h_E^{-1/2} \|v\|_{\omega_E} + h_E^{1/2} \|\nabla \tilde{v}_\ell\|_{\omega_E} + h_E^{1/2} \|\nabla v\|_{\omega_E}.$$

**Remark 4.6** There is a mesh size independent bounded number of edges satisfying (iv). More precisely, all these edges have an end point belonging to the triangle containing the crack tip.

**Proof:** (i). For both end points of  $E$ , we have:

$$|\pi_h v(x)| \lesssim h_x^{-1} \|v\|_{\omega_x} + \|\nabla v\|_{\omega_x}.$$

Writing  $\pi_h v = \sum_{x \in E} \pi_h v(x) \lambda_x$  and using  $\|\lambda_x\|_E \sim h_E^{1/2}$ ,  $h_E \leq h_x$  implies the result.

(ii). Suppose first that  $E$  lies in  $\Omega_\ell$ . Then  $E \cap \bar{\Omega}_\ell = E$  and for both end points of  $E$ , we have:

$$|\tilde{\pi}_h^\ell v(x)| \lesssim h_x^{-1} \|\tilde{v}_\ell\|_{\omega_x} + \|\nabla \tilde{v}_\ell\|_{\omega_x}.$$

The estimate is obtained as in (i). If  $E$  is cut by the crack the discussion is the same.

(iii) and (iv). Straightforward (see (i) and (ii)).  $\blacksquare$

Now we need to study the stability of the quasi-interpolation operator  $\pi_h$  on the crack. We denote by  $F_h \subset E_h$  the set of edges lying on the crack (these edges are the ones of the generalized elements on the crack).

**Lemma 4.7** For all  $v \in H^1(\Omega)$  and all edge  $F \in F_h$  one has:

(i) If  $F \subset T \in T_h$  where  $T$  is totally enriched, then for  $\ell = 1$  and  $\ell = 2$ , we have:

$$\|(\pi_h v)|_{\Omega_\ell}\|_F \lesssim h_F^{1/2} h_T^{-1} \|\tilde{v}_\ell\|_{\omega_T} + h_F^{1/2} \|\nabla \tilde{v}_\ell\|_{\omega_T},$$

(ii) If  $F \subset T \in T_h$  where  $T$  is partially enriched, then for  $\ell = 1$  and  $\ell = 2$ , we have:

$$\|(\pi_h v)|_{\Omega_\ell}\|_F \lesssim h_F^{1/2} h_T^{-1} \|\tilde{v}_\ell\|_{\omega_T} + h_F^{1/2} \|\nabla \tilde{v}_\ell\|_{\omega_T} + h_F^{1/2} h_T^{-1} \|v\|_{\omega_T} + h_F^{1/2} \|\nabla v\|_{\omega_T},$$

(iii) If  $F \subset T \in T_h$  where the crack tip lies in the interior of  $T$ , (then  $(\pi_h v)|_{\Omega_1} = (\pi_h v)|_{\Omega_2}$  on  $F$ ), we have:

$$\|\pi_h v\|_F \lesssim h_F^{1/2} h_T^{-1} \|v\|_{\omega_T} + h_F^{1/2} \|\nabla v\|_{\omega_T}.$$

**Proof:** Consider an edge  $F = (a, b)$  and fix  $\ell = 1$  or  $\ell = 2$ . On  $F$ , we have

$$(\pi_h v)|_{\Omega_\ell} = (\pi_h v)|_{\Omega_\ell}(a)\lambda_a + (\pi_h v)|_{\Omega_\ell}(b)\lambda_b,$$

where  $\lambda_a$  and  $\lambda_b$  are the edge basis functions at  $a$  and  $b$ . Let  $T = x_1x_2x_3 \in T_h$  be the triangle containing  $F$ . Since  $(\pi_h v)|_{\Omega_\ell}$  is constructed by the restriction of an affine extension on  $T$ , it is straightforward that  $(\pi_h v)|_{\Omega_\ell}(a)$  and  $(\pi_h v)|_{\Omega_\ell}(b)$  are convex combinations of  $\tilde{\pi}_h^\ell v(x_i)$  or  $\pi_h v(x_i)$  depending on the fact that  $x_i$  is enriched or not. So we have either:

$$|\tilde{\pi}_h^\ell v(x_i)| \lesssim h_{x_i}^{-1} \|\tilde{v}_\ell\|_{\omega_{x_i}} + \|\nabla \tilde{v}_\ell\|_{\omega_{x_i}},$$

or

$$|\pi_h v(x_i)| \lesssim h_{x_i}^{-1} \|v\|_{\omega_{x_i}} + \|\nabla v\|_{\omega_{x_i}}.$$

Using  $\|\lambda_a\|_F \sim \|\lambda_b\|_F \sim h_F^{1/2}$ , implies the result in (i), (ii) and (iii).  $\blacksquare$

### 4.3 Error estimates

We now consider the local error estimates in the  $L^2$ -norms.

**Lemma 4.8** *For all  $v \in H^1(\Omega)$  and all  $T \in T_h$  one has:*

(i) *if none of the nodes of  $T$  is enriched then*

$$\|v - \pi_h v\|_T \lesssim h_T \|\nabla v\|_{\omega_T},$$

(ii) *if the three nodes of  $T$  are enriched then for  $\ell = 1$  or  $\ell = 2$ , we have:*

$$\|v - \pi_h v\|_{T \cap \Omega_\ell} \lesssim h_T \|\nabla \tilde{v}_\ell\|_{\omega_T},$$

(iii) *if one or two nodes of  $T$  are enriched and if  $\omega_T$  is cut by the crack (so  $T \subset \bar{\Omega}_\ell$  for  $\ell = 1$  or  $\ell = 2$ ) we have:*

$$\|v - \pi_h v\|_T \lesssim h_T \|\nabla \tilde{v}_\ell\|_{\omega_T},$$

(iv) *if one or two nodes of  $T$  are enriched and if  $\omega_T$  contains the crack tip then for  $\ell = 1$  or  $\ell = 2$ , we have:*

$$\|v - \pi_h v\|_{T \cap \Omega_\ell} \lesssim h_T \sqrt{-\ln(h_T)} (\|\nabla \tilde{v}_\ell\|_\Omega + \|\nabla v\|_\Omega).$$

**Proof:** We first note that  $\pi_h$  preserves the constant functions (note that we can suppose that constant functions are extended on the other side of the crack by the same constant functions). Hence, for any  $v \in H^1(\Omega)$  and any constant function  $c(x) = c$  we can write:

$$v - \pi_h v = v - c - \pi_h(v - c).$$

(i) In this case

$$\|v - \pi_h v\|_T \leq \|v - c\|_{\omega_T} + \|\pi_h(v - c)\|_T \lesssim h_T \|\nabla v\|_{\omega_T},$$

where we use Lemma 4.3(i) and we choose  $c = |\omega_T|^{-1} \int_{\omega_T} v(x) dx$  together with  $h_T \sim h_{\omega_T}$ .

(ii) We write, for any constant function  $c$ :

$$\begin{aligned} \|v - \pi_h v\|_{T \cap \Omega_\ell} &\leq \|\tilde{v}_\ell - c\|_{\omega_T} + \|\pi_h(v - c)\|_{T \cap \Omega_\ell} \\ &\lesssim \|\tilde{v}_\ell - c\|_{\omega_T} + h_T \|\nabla \tilde{v}_\ell\|_{\omega_T} \\ &\lesssim h_T \|\nabla \tilde{v}_\ell\|_{\omega_T} \end{aligned}$$

where  $c = |\omega_T|^{-1} \int_{\omega_T} \tilde{v}_\ell(x) dx$  and we conclude as in (i) using Lemma 4.3(ii).

(iii) As the previous cases.

(iv) This estimate is obtained as follows using Lemma 4.3(iv) and choosing  $c = |\omega_T|^{-1} \int_{\omega_T} \tilde{v}_\ell(x) dx$ :

$$\begin{aligned} \|v - \pi_h v\|_{T \cap \Omega_\ell} &\leq \|\tilde{v}_\ell - c\|_{\omega_T} + \|\pi_h(v - c)\|_{T \cap \Omega_\ell} \\ &\lesssim \|\tilde{v}_\ell - c\|_{\omega_T} + \|v - c\|_{\omega_T} + h_T \|\nabla \tilde{v}_\ell\|_{\omega_T} + h_T \|\nabla v\|_{\omega_T} \\ &\lesssim \|\tilde{v}_\ell - v\|_{\omega_T} + h_T \|\nabla \tilde{v}_\ell\|_{\omega_T} + h_T \|\nabla v\|_{\omega_T}. \end{aligned}$$

Moreover, denoting by  $1_X$  the characteristic function of the set  $X$ , we write

$$\begin{aligned} \|\tilde{v}_\ell - v\|_{\omega_T} &= \|(\tilde{v}_\ell - v)1_{\omega_T}\|_{\Omega} \\ &\leq \|\tilde{v}_\ell - v\|_{L^q(\Omega)} \|1_{\omega_T}\|_{L^{\frac{2q}{q-2}}(\Omega)} \\ &\lesssim h_T^{1-\frac{2}{q}} \|\tilde{v}_\ell - v\|_{L^q(\Omega)} \\ &\lesssim q^{\frac{1}{2}} h_T^{1-\frac{2}{q}} \|\tilde{v}_\ell - v\|_{1,\Omega} \\ &\lesssim q^{\frac{1}{2}} h_T^{1-\frac{2}{q}} \|\nabla(\tilde{v}_\ell - v)\|_{\Omega} \\ &\lesssim q^{\frac{1}{2}} h_T^{1-\frac{2}{q}} (\|\nabla \tilde{v}_\ell\|_{\Omega} + \|\nabla v\|_{\Omega}) \end{aligned}$$

where  $2 < q < \infty$  and we used the Sobolev inequality  $\|w\|_{L^q(\Omega)} \leq Cq^{1/2} \|w\|_{1,\Omega}$ , see e.g. [16]. We obtain the final estimate by choosing  $q = -\ln(h_T)$ .  $\blacksquare$

**Lemma 4.9** For all  $v \in H^1(\Omega)$  and all edge  $E$  of a triangle  $T \in T_h$  one has:

(i) if both end points of  $E$  are not enriched:

$$\|v - \pi_h v\|_E \lesssim h_E^{1/2} \|\nabla v\|_{\omega_E},$$

(ii) if both end points of  $E$  are enriched then for  $\ell = 1$  or  $\ell = 2$ , we have:

$$\|v - \pi_h v\|_{E \cap \bar{\Omega}_\ell} \lesssim h_E^{1/2} \|\nabla \tilde{v}_\ell\|_{\omega_E},$$

(iii) if only one end point of  $E$  is enriched and if  $\omega_E$  is cut by the crack (so  $E \subset \bar{\Omega}_\ell$  for  $\ell = 1$  or  $\ell = 2$ ), we have:

$$\|v - \pi_h v\|_E \lesssim h_E^{1/2} \|\nabla \tilde{v}_\ell\|_{\omega_E},$$

(iv) if only one end point of  $E$  is enriched and if  $\omega_E$  contains the crack tip then for  $\ell = 1$  or  $\ell = 2$ , we have:

$$\|v - \pi_h v\|_{E \cap \bar{\Omega}_\ell} \lesssim h_E^{1/2} \sqrt{-\ln(h_E)} (\|\nabla \tilde{v}_\ell\|_{\Omega} + \|\nabla v\|_{\Omega}).$$

**Proof:** (i) Since  $\pi_h$  preserves the constant functions we have for all  $v \in H^1(\Omega)$  and all constant function  $c(x) = c$ :  $v - \pi_h v = v - c - \pi_h(v - c)$ . So by the scaled trace inequality (11) and Lemma 4.5(i), we obtain

$$\|v - \pi_h v\|_E \leq \|v - c\|_E + \|\pi_h(v - c)\|_E \lesssim h_E^{-1/2} \|v - c\|_{\omega_E} + h_E^{1/2} \|\nabla v\|_{\omega_E},$$

and we choose  $c = |\omega_E|^{-1} \int_{\omega_E} v(x) dx$  together with  $h_E \sim h_{\omega_E}$ .

(ii, iii) As in the previous cases.

(iv) This estimate is obtained as follows by using Lemma 4.5(iv) and choosing  $c = |\omega_E|^{-1} \int_{\omega_E} \tilde{v}_\ell(x) dx$ . We then achieve the same calculations as in Lemma 4.8(iv):

$$\begin{aligned} \|v - \pi_h v\|_{E \cap \bar{\Omega}_\ell} &\leq \|\tilde{v}_\ell - c\|_E + \|\pi_h(v - c)\|_{E \cap \bar{\Omega}_\ell} \\ &\lesssim h_E^{-1/2} \|\tilde{v}_\ell - c\|_{\omega_E} + h_E^{-1/2} \|v - c\|_{\omega_E} + h_E^{1/2} \|\nabla \tilde{v}_\ell\|_{\omega_E} + h_E^{1/2} \|\nabla v\|_{\omega_E} \\ &\lesssim h_E^{-1/2} \|\tilde{v}_\ell - v\|_{\omega_E} + h_E^{1/2} \|\nabla \tilde{v}_\ell\|_{\omega_E} + h_E^{1/2} \|\nabla v\|_{\omega_E} \\ &\lesssim h_E^{1/2} \sqrt{-\ln(h_E)} (\|\nabla \tilde{v}_\ell\|_\Omega + \|\nabla v\|_\Omega). \end{aligned}$$

■

The next lemma consists of estimating the error committed by the averaging operator on the edges of the generalized elements located on the crack. We recall that the set of such edges is denoted  $F_h$ .

**Lemma 4.10** *For all  $v \in H^1(\Omega)$  and all edge  $F \in F_h$  one has:*

(i) *If  $F \subset T \in T_h$  where  $T$  is totally enriched, then for  $\ell = 1$  and  $\ell = 2$ , we have:*

$$\|(v - \pi_h v)|_{\Omega_\ell}\|_F \lesssim h_T^{1/2} \|\nabla \tilde{v}_\ell\|_{\omega_T},$$

(ii) *If  $F \subset T \in T_h$  where  $T$  is partially enriched, then for  $\ell = 1$  and  $\ell = 2$ , we have:*

$$\|(v - \pi_h v)|_{\Omega_\ell}\|_F \lesssim h_T^{1/2} \sqrt{-\ln(h_T)} (\|\nabla \tilde{v}_\ell\|_\Omega + \|\nabla v\|_\Omega),$$

(iii) *If  $F \subset T \in T_h$  where the crack tip lies in the interior of  $T$ , (then  $(\pi_h v)|_{\Omega_1} = (\pi_h v)|_{\Omega_2}$  on  $F$ ), we have:*

$$\|v|_{\Omega_\ell} - \pi_h v\|_F \lesssim h_T^{1/2} \|\nabla v\|_{\omega_T}.$$

**Proof:** (i) Since  $\pi_h$  preserves the constant functions we have for all  $v \in H^1(\Omega)$  and all constant function  $c(x) = c$ :  $v - \pi_h v = v - c - \pi_h(v - c)$ . By the generalized scaled trace inequality (see [17, 19]):

$$\|w\|_F \lesssim h_T^{-1/2} \|w\|_T + h_T^{1/2} \|\nabla w\|_T,$$

and Lemma 4.7, we obtain

$$\begin{aligned} \|(v - \pi_h v)|_{\Omega_\ell}\|_F &\leq \|\tilde{v}_\ell - c\|_F + \|\pi_h(\tilde{v}_\ell - c)\|_F \\ &\lesssim h_T^{-1/2} \|\tilde{v}_\ell - c\|_T + h_T^{1/2} \|\nabla \tilde{v}_\ell\|_T + h_F^{1/2} h_T^{-1} \|\tilde{v}_\ell - c\|_{\omega_T} + h_F^{1/2} \|\nabla \tilde{v}_\ell\|_{\omega_T}. \end{aligned}$$

Hence the conclusion. The proof of (ii) and (iii) are the same as previously. ■

Having defined and analyzed the quasi-interpolation operator  $\pi_h : X \rightarrow X_h$  in the scalar case, the extension to the vector valued case is straightforward: we define

$$\pi_h^* : V = X \times X \rightarrow X_h \times X_h$$

such that for any  $v = (v_1, v_2) \in X \times X$  we have  $\pi_h^* v = (\pi_h v_1, \pi_h v_2)$ . Of course the error estimates in Lemmas 4.8, 4.9 and 4.10 also hold for  $\pi_h^*$ .

## 5 Error estimators

### 5.1 Definition of the residual error estimators

Writing  $u_h = u_{h,r} + \chi u_{h,s}$  as in (5), the element residual is defined by

$$R_G = f + \operatorname{div} \sigma(u_h) = f + \operatorname{div} \sigma(\chi u_{h,s})$$

on each generalized element  $G \in G_h$ . Since  $\operatorname{div} \sigma(u_{h,s}) = 0$  we deduce that the expression  $\operatorname{div} \sigma(\chi u_{h,s})$  vanishes excepted on the elements (distant from the crack tip) having a nonempty intersection with the ring shaped area where  $\chi$  maps onto  $(0, 1)$ . To simplify we denote by  $n$  instead of  $n_E$  the normal vectors to the elements on the edges  $E$ .

**Definition 5.1 (Residual error estimator)** *Let  $G \in G_h$  and  $T \in T_h$  be the triangle containing  $G$ . The local and global residual error estimators are defined by*

$$\begin{aligned} \eta_{1G} &= h_T C(h_T) \|f + \operatorname{div} \sigma(\chi u_{h,s})\|_G, \\ \eta_{2G} &= h_T^{1/2} D(h_T) \left( \sum_{E \in E_G^{\text{int}} \cup E_G^N \cup E_G^C} \|[\sigma(u_h)n]_E\|_E^2 \right)^{1/2}, \\ \eta_G &= (\eta_{1G}^2 + \eta_{2G}^2)^{1/2}, \\ \eta &= \left( \sum_{G \in G_h} \eta_G^2 \right)^{1/2}, \end{aligned}$$

where  $C(h_T) = \sqrt{-\ln(h_T)}$  for the elements in case (iv) of Lemma 4.8, otherwise  $C(h_T) = 1$  and  $D(h_T) = \sqrt{-\ln(h_T)}$  for the elements in case (iv) of Lemma 4.9 or in case (ii) of Lemma 4.10, otherwise  $D(h_T) = 1$ .

**Remark 5.2** *The presence of the  $\ln(h_T)$ -terms in the estimator results from technical reasons and appears only for a bounded number (independent of the mesh) of elements near the crack tip. From a numerical point of view, these  $\ln(h_T)$ -terms are negligible. In the case of a standard finite element method with coinciding finite element meshes on the crack we have  $G_h = T_h$  and  $G = T$  (obviously the XFEM is not a generalization of a standard finite element method with noncoinciding finite element meshes on the crack). In the case of coinciding meshes on the crack it is easy to show that the cases involving the  $\ln(h_T)$ -terms disappear (i.e.,  $C(h_T) = D(h_T) = 1$ ) and we recover the classical residual estimator (see e.g., [4, 31]).*

### 5.2 Upper error bound

**Theorem 5.3** *Let  $u \in V$  be the solution of (2) and let  $u_h \in V_h$  be the solution of (7). Then*

$$\|u - u_h\|_{1,\Omega} \lesssim \eta.$$

**Proof:** Denoting the error by

$$e = u - u_h,$$

we have, according to (2), (7) and Korn inequality:

$$\begin{aligned}
\|e\|_{1,\Omega}^2 &\lesssim \int_{\Omega} \sigma(u) : \varepsilon(u - u_h) - \int_{\Omega} \sigma(u_h) : \varepsilon(u - u_h) \\
&= \int_{\Omega} f \cdot (u - u_h) - \int_{\Omega} \sigma(u_h) : \varepsilon(u - u_h) \\
&= \int_{\Omega} f \cdot (u - v_h) - \int_{\Omega} \sigma(u_h) : \varepsilon(u - v_h), \quad \forall v_h \in V_h.
\end{aligned}$$

Splitting up the integrals on each generalized element  $G \in G_h$  and writing  $u_h = u_{h,r} + \chi u_{h,s}$ , we arrive at

$$\begin{aligned}
\|e\|_{1,\Omega}^2 &\lesssim \sum_{G \in G_h} \int_G f \cdot (u - v_h) \\
&\quad - \sum_{G \in G_h} \int_G \sigma(u_{h,r}) : \varepsilon(u - v_h) - \sum_{G \in G_h} \int_G \sigma(\chi u_{h,s}) : \varepsilon(u - v_h) \\
&= \sum_{G \in G_h} \int_G (f + \operatorname{div} \sigma(\chi u_{h,s})) \cdot (u - v_h) \\
(14) \quad &- \sum_{E \in E_h^{int}} \int_E [\sigma(u_{h,r})n]_E \cdot (u - v_h) - \sum_{E \in E_h^N \cup E_h^C} \int_E \sigma(u_h)n \cdot (u - v_h), \quad \forall v_h \in V_h,
\end{aligned}$$

where we used the Green formula on each generalized element (note that although the triangle containing the crack tip has a boundary which is not Lipschitz, it can be divided in two parts by using a straight extension of the crack and then one can use separately Green's formula on each part to obtain the desired result) as well as  $\operatorname{div} \sigma(u_{h,r}) = 0$  on  $G$  and  $[\sigma(\chi u_{h,s})n]_E = 0$  for all  $E \in E_h^{int}$ .

At this stage we fix the choice of  $v_h$ . We set

$$v_h = u_h + \pi_h^*(u - u_h).$$

We consider (14): with the above choice we are able to estimate each term of the right-hand side of the previous expression. Cauchy-Schwarz inequality implies

$$\sum_{G \in G_h} \int_G (f + \operatorname{div} \sigma(\chi u_{h,s})) \cdot (u - v_h) \leq \sum_{G \in G_h} \|f + \operatorname{div} \sigma(\chi u_{h,s})\|_G \|u - v_h\|_G.$$

Therefore it remains to estimate  $\|u - v_h\|_G$  for any generalized element  $G$ . Let  $T \in T_h$  be the triangle containing  $G$ . Using Lemma 4.8, we obtain for the triangles considered in cases (i)–(iii):

$$(15) \quad \|u - v_h\|_G = \|e - \pi_h^* e\|_G \lesssim h_T \|e\|_{1,\omega_T}$$

or

$$(16) \quad \|u - v_h\|_G = \|e - \pi_h^* e\|_G \lesssim h_T \|\tilde{e}\|_{1,\omega_T},$$

where  $\tilde{e}$  is an extension of the error across the crack (see (8), (9)). If  $T$  belongs to the finite set of triangles (iv) in Lemma 4.8, we have

$$(17) \quad \|u - v_h\|_G = \|e - \pi_h^* e\|_G \lesssim h_T \sqrt{-\ln(h_T)} (\|\tilde{e}\|_{1,\Omega} + \|e\|_{1,\Omega}).$$

So, depending on the cases (i)–(iv) of Lemma 4.8 and using estimates (15)–(17), we can write

$$\begin{aligned}
(18) \quad & \sum_{G \in G_h} \int_G (f + \operatorname{div} \sigma(\chi u_{h,s})) \cdot (u - v_h) \\
& \lesssim \left( \sum_{G \in G_h, \text{cases}(i)-(iii)} h_T^2 \|f + \operatorname{div} \sigma(\chi u_{h,s})\|_G^2 \right)^{1/2} \left( \sum_{G \in G_h, \text{cases}(i)-(iii)} (\|\tilde{e}\|_{1,\omega_T} + \|e\|_{1,\omega_T})^2 \right)^{1/2} \\
& \quad + \left( \sum_{G \in G_h, \text{case}(iv)} h_T^2 (-\ln(h_T)) \|f + \operatorname{div} \sigma(\chi u_{h,s})\|_G^2 \right)^{1/2} \left( \sum_{G \in G_h, \text{case}(iv)} (\|\tilde{e}\|_{1,\Omega} + \|e\|_{1,\Omega})^2 \right)^{1/2} \\
& \lesssim \eta \|e\|_{1,\Omega}.
\end{aligned}$$

Let us now pass to the estimate of the remaining terms: as above the application of Cauchy-Schwarz inequality leads to

$$\begin{aligned}
& - \sum_{E \in E_h^{\text{int}}} \int_E \llbracket \sigma(u_{h,r}) n \rrbracket_E \cdot (u - v_h) - \sum_{E \in E_h^N \cup E_h^C} \int_E \sigma(u_h) n \cdot (u - v_h) \\
& = - \sum_{E \in E_h^N \cup E_h^{\text{int}} \cup E_h^C} \int_E \llbracket \sigma(u_h) n \rrbracket_E \cdot (e - \pi_h^* e) \\
(19) \quad & \leq \sum_{E \in E_h^N \cup E_h^{\text{int}} \cup E_h^C} \|\llbracket \sigma(u_h) n \rrbracket_E\|_E \|e - \pi_h^* e\|_E.
\end{aligned}$$

Using Lemmas 4.9 (i,ii,iii) and 4.10 (i,iii) and denoting by  $T \in T_h$  a triangle containing  $E$ , we obtain

$$(20) \quad \|e - \pi_h^* e\|_E \lesssim h_T^{1/2} (\|\tilde{e}\|_{1,\omega_T} + \|e\|_{1,\omega_T}).$$

If  $E$  belongs to the finite set of triangles in Lemma 4.9(iv) or in Lemma 4.10(ii), we have

$$(21) \quad \|e - \pi_h^* e\|_E \lesssim h_T^{1/2} \sqrt{-\ln(h_T)} (\|\tilde{e}\|_{1,\Omega} + \|e\|_{1,\Omega}).$$

Using estimates (20) and (21) with (19) as well as (18) ends the proof of the theorem.  $\blacksquare$

## 6 Numerical experiments

In this section we implement the residual estimator of Definition 5.1 on three examples using Getfem++ (see [26]). We suppose that the body  $\Omega$  is homogeneous isotropic so that Hooke's law  $\sigma(v) = C\varepsilon(v)$  becomes

$$\sigma(v) = \lambda \operatorname{tr}(\varepsilon(v)) I + 2\mu \varepsilon(v)$$

where  $I$  represents the identity matrix,  $\operatorname{tr}$  is the trace operator,  $\lambda \geq 0$  and  $\mu > 0$  denote the Lamé coefficients.



## 6.1 The opening mode (Mode I)

In the first example we choose the domain  $\Omega = (0, 1)^2$  depicted in Figure 5 with a crack  $[0, 0.5] \times \{0.5\}$  and  $\Gamma_N = \emptyset$ . Here the mesh coincides with the crack so that  $T_h = G_h$ . We impose nonhomogeneous Dirichlet conditions on the boundary  $\Gamma_D$ . The coefficients of Lamé are  $\lambda = 200$  and  $\mu = 150$ . The cutoff function  $\chi$  in (6) is chosen polynomial of degree five with  $r_0 = 0.01$  and  $r_1 = 0.49$  and it is defined by

$$\chi(r) = \frac{-6r^5 + 15(r_0 + r_1)r^4 - 10(r_0^2 + 4r_0r_1 + r_1^2)r^3 + 30r_0r_1(r_0 + r_1)r^2 - 30r_1^2r_0^2r + r_0^3(r_0^2 - 5r_1r_0 + 10r_1^2)}{(r_1 - r_0)^5}$$

if  $r_0 \leq r \leq r_1$ .

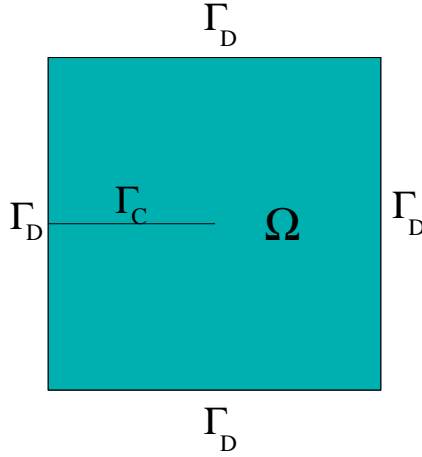


Figure 5: First example. The cracked body

### 6.1.1 Uniform refinement

The domain is discretized with a family of uniform triangular meshes. In the following we denote by  $N_D$  the number of elements of the mesh on a side of the square  $(0, 1)^2$ . Since we use uniform meshes, the parameter  $N_D$  measures the size of the mesh. The exact solution  $u = u_I$  is known (given by (3)) so we can evaluate the norm  $\|u - u_h\|_{1,\Omega}$  and consequently the effectivity index which is equal to  $\eta/\|u - u_h\|_{1,\Omega}$  (see Table 1).

$N_D$	8	16	32	48	64	80	96	112	128
$\eta (\times 10^{-2})$	7.48248	4.34222	2.46972	1.74772	1.35644	1.10928	0.938618	0.813512	0.717829
$\ u - u_h\ _{1,\Omega}$ ( $\times 10^{-4}$ )	6.99878	4.39294	2.4652	1.71217	1.31164	1.06293	0.893545	0.770712	0.677583
Effectivity index	106.91	98.84	100.18	102.07	103.41	104.36	105.04	105.55	105.93

Table 1: Values of  $\eta$ ,  $\|u - u_h\|_{1,\Omega}$  and effectivity index for the first example.

Figure 6 depicts the convergence rates of  $\eta$  and  $\|u - u_h\|_{1,\Omega}$  of Table 1. The error estimator  $\eta$  admits a similar convergence rate as the error norm  $\|u - u_h\|_{1,\Omega}$  and the convergence behaves (up to a constant) like  $h$  as the discretization parameter vanishes.

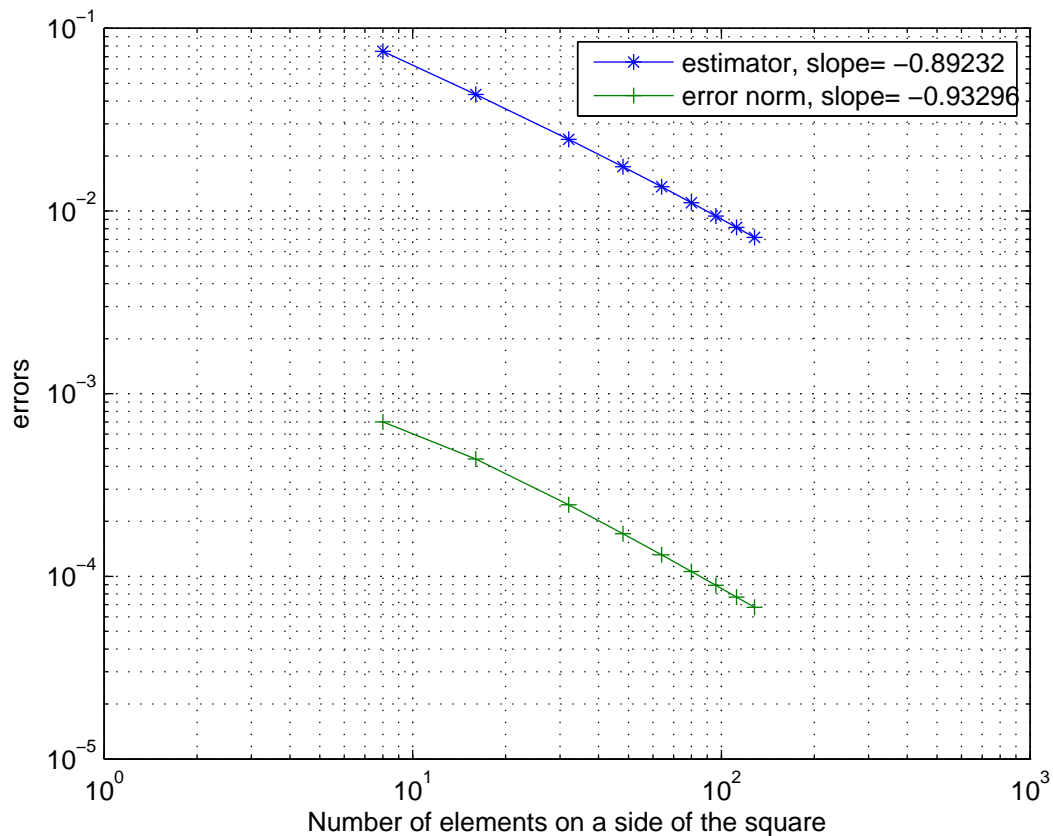


Figure 6: Convergence of the estimator  $\eta$  and of the error norm  $\|u - u_h\|_{1,\Omega}$

The main part of the error in  $\eta$  is located near the crack tip  $(0.5, 0.5)$  (see Figure 7).

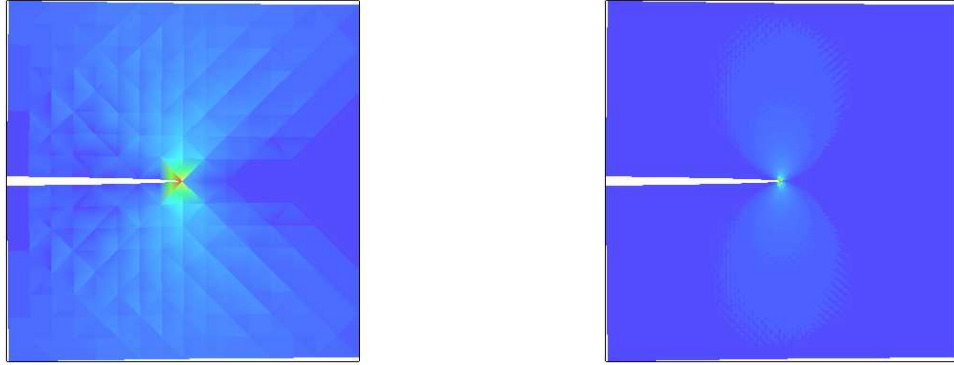


Figure 7: Map of the local error estimators  $\eta_G$  with  $N_D = 16$  (left) and  $N_D = 80$  (right)

### 6.1.2 Refinement with a threshold

Now we use the error estimator with an adaptive mesh refinement procedure. The criterion to refine the mesh is as follows: we define a threshold and the element  $G$  is refined if  $\eta_G$  is greater than the threshold. Mesh refinement is stopped as soon as  $\eta_G$  is lower than the threshold for any  $G$ . A initial uniform mesh is chosen. Taking a threshold of  $10^{-5}$  or of  $10^{-6}$  and an exponential cutoff function  $\chi(r) = \exp(-2075r^4)$  in  $\Omega$  leads to the meshes depicted in Figure 8. Choosing now as cutoff  $\chi$  the previously defined polynomial function of degree five leads to the meshes in Figure 9. Finally the error estimator  $\eta$  obtained at each intermediate mesh with a threshold equal to  $10^{-6}$  is reported in Table 2 (for the exponential cutoff function) and in Table 3 (for the polynomial cutoff function of degree five). In this example the different cutoff functions lead to different refined meshes with a satisfactory error reduction in both cases.

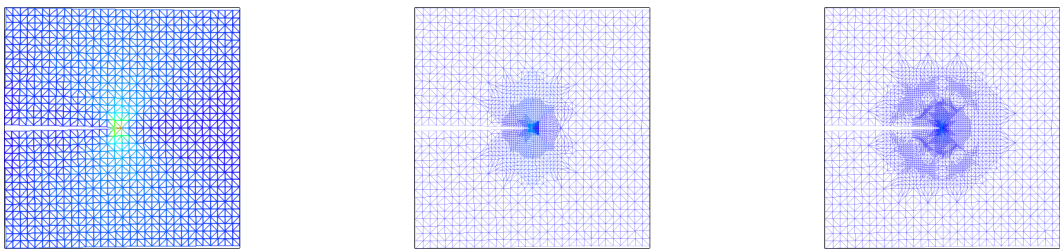


Figure 8: Case of an exponential cutoff function  $\chi$ : initial mesh (left), final mesh with a threshold equal to  $10^{-5}$  (middle) and final mesh with a threshold equal to  $10^{-6}$  (right)

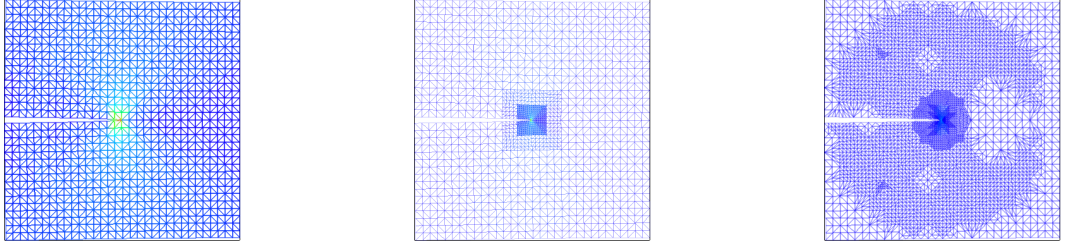


Figure 9: Case of a polynomial cutoff function  $\chi$  of degree five: initial mesh (left), final mesh with a threshold equal to  $10^{-5}$  (middle) and final mesh with a threshold equal to  $10^{-6}$  (right)

Degrees of freedom	730	1106	1472	1500	1526
$\eta (\times 10^{-2})$	4.45143	2.94918	2.07349	1.91532	1.82311

Table 2: Values of  $\eta$  with an exponential cutoff function  $\chi$

Degrees of freedom	730	1666	1714	1734	1740
$\eta (\times 10^{-2})$	4.34222	2.30949	2.04415	1.93209	1.90008

Table 3: Values of  $\eta$  with a polynomial cutoff function  $\chi$  of degree five

## 6.2 The shear mode (Mode II)

### 6.2.1 Uniform refinement

We choose the same geometry and material characteristics as the previous example. But now the exact solution  $u = u_{II}$  is given by (4). In Table 4, we report the contributions of  $\eta$ ,  $\|u - u_h\|_{1,\Omega}$  and the effectivity indexes for a family a uniform triangular meshes.

$N_D$	8	16	32	48	64	80	96	112	128
$\eta (\times 10^{-2})$	8.65243	4.64238	2.44897	1.6639	1.26226	1.01857	0.855114	0.73785	0.649653
$\ u - u_h\ _{1,\Omega}$ ( $\times 10^{-4}$ )	9.24249	5.68551	3.14573	2.17081	1.65698	1.33966	1.12436	0.968637	0.850816
Effectivity index	93.62	81.65	77.85	76.64	76.17	76.03	76.05	76.17	76.35

Table 4: Values of  $\eta$ ,  $\|u - u_h\|_{1,\Omega}$  and effectivity index for the second example.

We report the convergence rates of  $\eta$  and  $\|u - u_h\|_{1,\Omega}$  in Figure 10. The conclusions are the same as in the first example: the estimator and the  $H^1$ -error norm are of order  $h$  as  $h \rightarrow 0$ . Moreover the main part of the error in  $\eta$  is still located near the crack tip  $(0.5, 0.5)$  (see Figure 11).

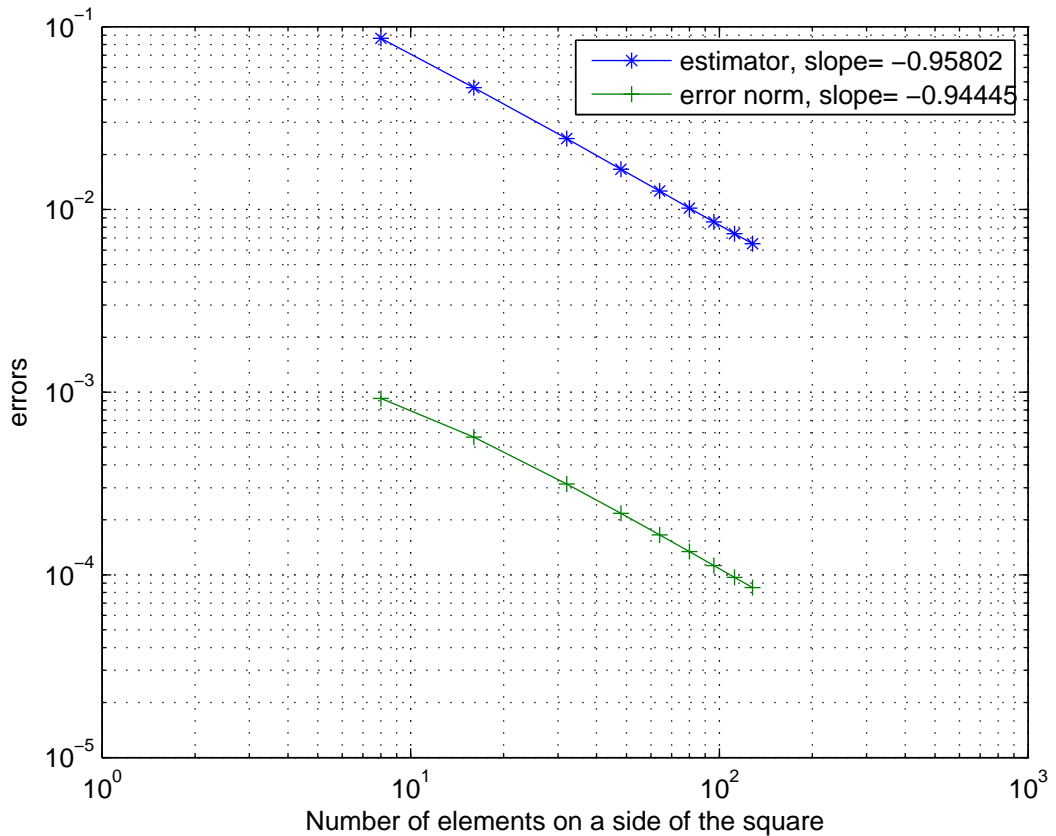


Figure 10: Convergence of the estimator  $\eta$  and of the error norm  $\|u - u_h\|_{1,\Omega}$

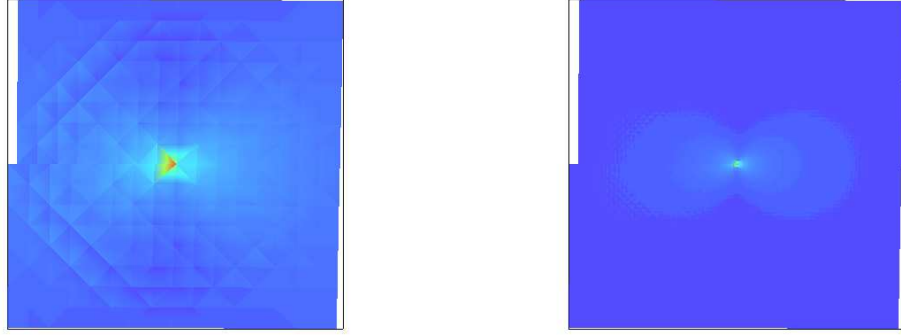


Figure 11: Map of local error estimators  $\eta_G$  with  $N_D = 16$  (left) and  $N_D = 80$  (right)

### 6.2.2 Refinement with a threshold

The criterion to refine the mesh is the same as before. The initial and final meshes using an exponential cutoff function for two different thresholds are depicted in Figure 12. Figure 13 depicts the same quantities when a polynomial cutoff function of degree five is used. Finally the error estimator  $\eta$  obtained at each intermediate mesh with a threshold equal to  $10^{-6}$  is reported in Table 5 (for the exponential cutoff function) and in Table 6 (for the polynomial cutoff function of degree five).

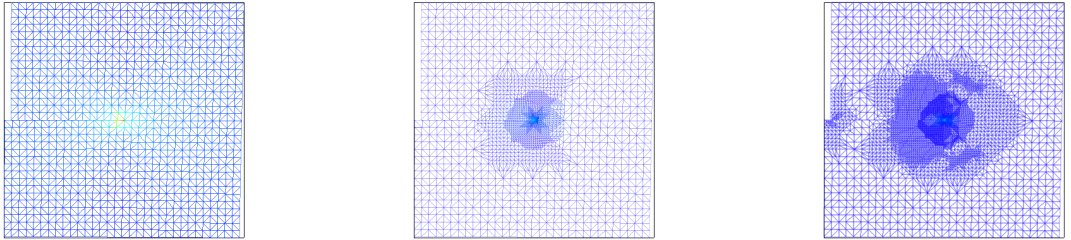


Figure 12: Case of an exponential cutoff function  $\chi$ : initial mesh (left), final mesh with a threshold equal to  $10^{-5}$  (middle) and final mesh with a threshold equal to  $10^{-6}$  (right)

Degrees of freedom	730	1146	1782	1808	1850	1880
$\eta (\times 10^{-2})$	5.50767	3.87577	2.45115	2.26363	2.08548	2.07013

Table 5: Values of  $\eta$  with an exponential cutoff function  $\chi$

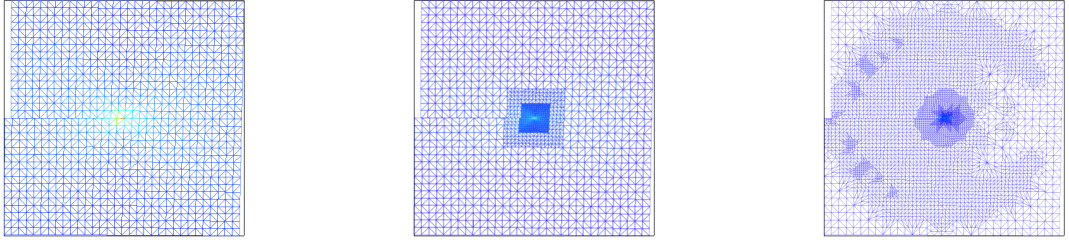


Figure 13: Case of a polynomial cutoff function  $\chi$  of degree five: initial mesh (left), final mesh with a threshold equal to  $10^{-5}$  (middle) and final mesh with a threshold equal to  $10^{-6}$  (right)

Degrees of freedom	730	1668	1848	1874	1944
$\eta (\times 10^{-2})$	4.64238	2.97789	2.49811	2.32357	2.08207

Table 6: Values of  $\eta$  with a polynomial cutoff function  $\chi$  of degree five

### 6.3 The L-shaped body:

In the third example, we consider a cracked L-shaped body (which corresponds to three quarters of the square  $(0,1)^2$ ) represented in Figure 14. The crack tip is located at  $(0.375, 0.25)$ . Now the mesh doesn't coincide with the crack. We set  $\Gamma_D = (0, 0.5) \times \{1\}$  and  $\Gamma_N$  elsewhere. A density of surface forces  $F=(0,-1)$  is applied on  $\Gamma_{N1} = (0, 1) \times \{0\} \subset \Gamma_N$  and  $N$  stands for the number of elements of the mesh on  $\Gamma_D$ . The material characteristics and the cutoff function are the same as in the previous examples.

#### 6.3.1 Uniform refinement

In this example, we don't have at our disposal the exact solution. Therefore we only report the values of  $\eta$  in Table 7 when using a family of uniform triangular meshes.

$N$	8	16	32	48	64	80	96
$\eta (\times 10^{-2})$	28.1005	15.7341	8.323	5.69931	4.34828	3.52219	2.96384

Table 7: Values of  $\eta$  for the third example

We observe in Figure 15 that the convergence rate of the estimator is close to one and it is therefore similar to the ones in the previous examples. The main part of the error in  $\eta$  is located near the crack tip  $(0.375, 0.25)$  (see Figure 16).

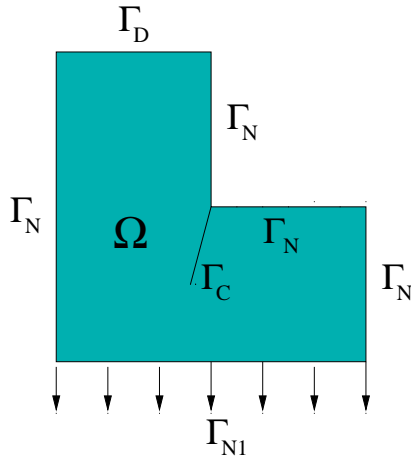


Figure 14: Third example. The cracked body

### 6.3.2 Refinement with a threshold

Using the same mesh refinement criterion as in the previous examples, we report the initial and two final meshes using an exponential cutoff function in Figure 17. The initial and two final meshes for a polynomial cutoff function of degree five are depicted in Figure 18. Finally the error estimator  $\eta$  obtained at each intermediate mesh with a threshold equal to  $10^{-5}$  is reported in Table 8 (for the exponential cutoff function) and in Table 9 (for the polynomial cutoff function of degree five).

Degrees of freedom	1740	2978	3242	3296	3316
$\eta$	0.195918	0.131541	0.113071	0.105575	0.103496

Table 8: Values of  $\eta$  with an exponential cutoff function  $\chi$

Degrees of freedom	1740	3156	3244	3312	3326
$\eta$	0.157341	0.117158	0.108942	0.103859	0.102766

Table 9: Values of  $\eta$  with a polynomial cutoff function  $\chi$  of degree five



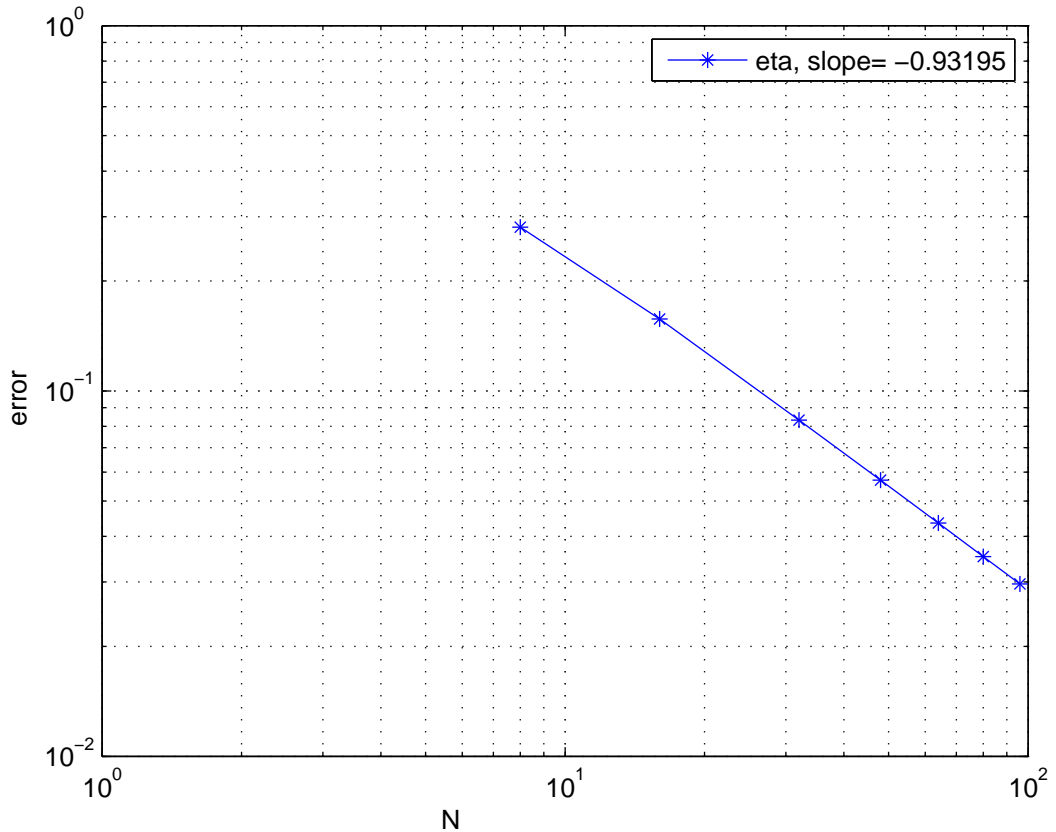


Figure 15: Convergence of the estimator  $\eta$

## 7 Conclusion

We propose, study and implement numerically a residual a posteriori error estimator for the two dimensional elasticity system approximated by XFEM. The estimator is a generalization of the existing one in the case of a classical finite element method with standard meshes. An upper bound of the  $H^1$ -error norm is obtained and the numerical experiments show that the estimator and the  $H^1$ -error norm admit similar convergence rates.

This work is supported by "l'Agence Nationale de la Recherche", project ANR-05-JCJC-0182-01.

## References

- [1] R.A. Adams, *Sobolev spaces*, Academic Press, 1975.
- [2] I. Babuška and W. Rheinboldt, Error estimates for adaptive finite element computations, *SIAM J. Numer. Anal.*, 15 (1978) 736–754.
- [3] C. Bernardi and V. Girault, A local regularisation operator for triangular and quadrilateral finite elements, *SIAM J. Numer. Anal.*, 35 (1998) 1893–1916.

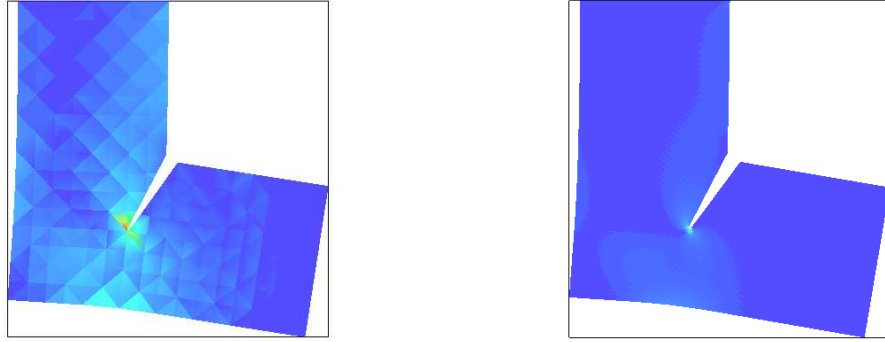


Figure 16: Map of the local error estimators  $\eta_G$  with  $N = 8$  (left) and  $N = 48$  (right)

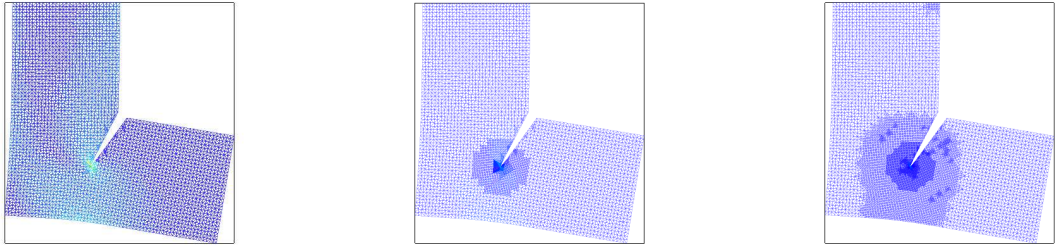


Figure 17: Case of an exponential cutoff function  $\chi$ : initial mesh (left), final mesh with a threshold equal to  $2 \times 10^{-4}$  (middle) and final mesh with a threshold equal to  $10^{-5}$  (right)

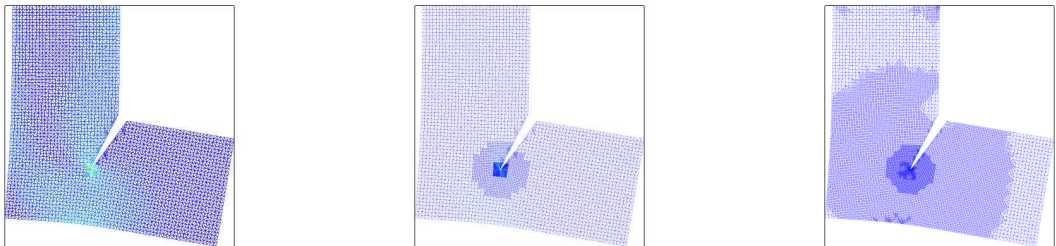


Figure 18: Case of a polynomial cutoff function  $\chi$  of degree five: initial mesh (left), final mesh with a threshold equal to  $2 \times 10^{-4}$  (middle) and final mesh with a threshold equal to  $4 \times 10^{-6}$  (right)

- [4] C. Bernardi, B. Métivet and R. Verfürth, *Analyse numérique d'indicateurs d'erreur*, Report 93025, Laboratoire d'analyse numérique, Université Paris VI, 1993.
- [5] S. Bordas and M. Duflot, Derivative recovery and a posteriori error estimate for extended finite elements, *Comput. Methods Appl. Mech. Engrg.*, 196 (2007) 3381–3399.
- [6] S. Bordas and M. Duflot, A posteriori error estimation for extended finite elements by an extended global recovery, *Int. J. Numer. Meth. Engrg.*, 76 (2008) 1123–1138.
- [7] S. Bordas, M. Duflot and P. Le, A simple error estimator for extended finite elements, *Commun. Numer. Meth. Engrg*, 24 (2008) 961–971.
- [8] S.C. Brenner and L.R. Scott, The mathematical theory of finite element methods, Springer-Verlag, 2002.
- [9] E. Chahine, P. Laborde and Y. Renard, A quasi-optimal convergence result for fracture mechanics with XFEM, *C. R. Acad. Sci. Paris*, 342 (2006) 527–532.
- [10] E. Chahine, P. Laborde and Y. Renard, Crack tip enrichment in XFEM using a cut-off function, *Int. J. Numer. Meth. Engrg.*, 75 (2008) 629–646.
- [11] Z. Chen and R.H. Nochetto, Residual type a posteriori error estimates for elliptic obstacle problems, *Numer. Math.*, 84 (2000) 527–548.
- [12] P.G. Ciarlet, The finite element method for elliptic problems, in *Handbook of Numerical Analysis*, Volume II, Part 1, Eds. P.G. Ciarlet and J.-L. Lions, North Holland, 17–352, 1991.
- [13] P. Clément, Approximation by finite element functions using local regularization, *RAIRO Anal. Numer.*, 2 (1975) 77–84.
- [14] A. Ern and J.-L. Guermond, Éléments finis : théorie, applications, mise en oeuvre, Springer-Verlag, 2001.
- [15] L. Evans, Partial differential equations, American Mathematical Society, 1999.
- [16] H. Fujita and T. Suzuki, Evolution problems, in *Handbook of Numerical Analysis*, Volume II, Part 1, Eds. P.G. Ciarlet and J.-L. Lions, North Holland, 791–927, 1991.
- [17] P. Grisvard, Elliptic problems in nonsmooth domains, Pitman, 1985.
- [18] P. Grisvard, Problèmes aux limites dans les polygones - mode d'emploi. *EDF Bull. Direction Etudes Rech. Sér. C. Math. Inform.*, 1 (1986) 21–59.
- [19] J. Haslinger and Y. Renard, A new fictitious domain approach inspired by the extended finite element method. *Siam J. Numer. Anal.*, 47 (2009) 1474–1499.
- [20] S. Hilbert, A mollifier useful for approximations in Sobolev spaces and some applications to approximating solutions of differential equations, *Math. Comp.*, 27 (1973) 81–89.
- [21] P. Hild, V. Lleras and Y. Renard, A posteriori error analysis for Poisson's equation approximated by XFEM, *Esaim Proceedings*, 27 (2009) 107–121.

- [22] J. Lemaitre, J.-L. Chaboche, Mechanics of Solid Materials, Cambridge University Press, 1994.
- [23] N. Moës and T. Belytschko, XFEM: nouvelles frontières pour les éléments finis, *Revue européenne des éléments finis (Calcul des structures GIENS'01)*, 11 (2002) 305–318.
- [24] N. Moës, J. Dolbow and T. Belytschko, A finite element method for cracked growth without remeshing , *Int. J. Numer. Meth. Engrg.*, 46 (1999) 131–150.
- [25] S. Nicaise, Y. Renard and E. Chahine, Optimal convergence analysis for the eXtended Finite Element Method, submitted.
- [26] Y. Renard and J. Pommier. *Getfem++*. An open source generic C++ library for finite element methods, <http://home.gna.org/getfem>.
- [27] J. J. Rodenas, O. A. Gonzales-Estrada and J. E. Tarancon, A recovery-type error estimator for the extended finite element method based on singular plus smooth stress field splitting, *Int. J. Numer. Meth. Engrg.*, 76 (2008) 545–571.
- [28] L.R. Scott and S. Zhang, Finite element interpolation of nonsmooth functions satisfying boundary conditions, *Math. Comp.*, 54 (1990) 483–493.
- [29] G. Strang, Approximation in the finite element method, *Numer. Math.*, 19 (1972) 81–98.
- [30] G. Strang, G. Fix, An analysis of the finite element method, Prentice-Hall, 1973.
- [31] R. Verfürth, A review of a posteriori error estimation and adaptative mesh refinement techniques, Wiley and Teubner, 1996.